Exotic superconductivity through bosons in a dynamical cluster approximation

Thomas Bilitewski and Lode Pollet

Exotic Superconductivity Through Bosons in a Dynamical Cluster Approximation

Thomas Bilitewski[*]

T.C.M. Group, Cavendish Laboratory, J.J. Thomson Avenue, Cambridge CB3 0HE, United Kingdom

Lode Pollet

Department of Physics, Arnold Sommerfeld Center for Theoretical Physics, and Center for Nanoscience,
Ludwig-Maximilians-Universität München, Theresienstraße 37, 80333 Munich, Germany

We study the instabilities towards (exotic) superconductivity of mixtures of spin-1/2 fermions coupled to scalar bosons on a two-dimensional square lattice with the Dynamical-Cluster-Approximation (DCA) using a numerically exact continuous-time Monte-Carlo solver. The Bogoliubov bosons provide an effective phononic bath for the fermions and induce a non-local retarded interaction between the fermions, which can lead to (exotic) superconductivity. Because of the sign problem the biggest clusters we can study are limited to 2×2 in size, but this nevertheless allows us to study the pairing instablilities, and their possible divergence, in the s- and d-wave channels as well as the competition with antiferromagnetic fluctuations. At fermionic half-filling we find that d-wave is stable when the mediated interaction by the bosons is of the same order as the bare fermionic repulsion. Its critical temperature can be made as high as the maximum one for s-wave, which opens perspectives for its detection in a cold atom experiment.

I. INTRODUCTION

Mixtures of bosons and fermions are ubiquitous: They are fundamental in particle physics, where bosons are the carriers of forces between fermionic matter particles. In condensed matter systems, they appear in the context of superconductivity, where the conventional pairing mechanism consists of phonons inducing an effective retarded attractive interaction between electrons leading to the formation of Cooper-pairs, as well as in mixtures of ^{3}He and ^{4}He in which the inter- and intra-isotope interactions are of comparable magnitude. Cold-atom systems are uniquely suited to simulate this physics as they allow fine experimental control over the interactions as well as the tunelling amplitudes[1,2].

The optical lattice system does not have phonons. Nevertheless, pairing mechanisms with cold fermions in an optical lattice can be investigated by quantum simulation. Bosons deep in the superfluid phase have a linear dispersion [3] which can play the role of phonons as in conventional superconductors (when fermions form an electron gas) but, as we will see, they can equally well couple to spin density wave fluctuations (relevant when the charge of the fermions is near localization). Spin density wave fluctuations induce an attractive interaction between electrons in a spin-singlet, with the pair wavefunction changing sign between different regions of the Fermi surface[4–13]. It plays a prominent role in the cuprates (where it correctly predicts d-wave pairing), the iron superconductors and heavy fermion materials[14–23]. The fermionic Hubbard repulsion and the lattice dispersion can, in principle, be changed in a cold-atom experiment and allow to systematically investigate the interplay of both pairing mechanisms.

Quantum degenerate mixtures of bosonic and spin-polarized fermionic species have first been realized experimentally with ^{23}Na and ^{6}Li[24]. Since then a variety of different species combinations have been employed in experiments and these systems have been studied extensively[25–45]. Recently, using ^{6}Li and ^{7}Li a system has been realised experimentally for the first time in which both bosonic and spinful fermionic species are superfluid[46], giving rise to induced interactions in the bosonic sector due to excitations of the fermionic superfluid[47,48]. Another promising candidate for experiments with spinful mixtures are ^{23}Na and ^{40}K in which a large number of interspecies Feshbach resonances at experimentally accessible magnetic fields have been identified enabling the tuning of the interspecies interactions and the simulation of boson-induced interactions between the fermions[49,50] and the creation of stable fermionic Feshbach molecules[51].

Theoretically, the interactions mediated by superfluid bosons [52] were studied in the regime where the sound velocity of the bosons is fast compared to the Fermi velocity and found to be attractive and capable of overcoming a sufficiently weak repulsive fermi interactions leading to s-wave pairing both in the continuum[52–60] and in optical lattices[3,61,62]. Recently, the phase diagram of Bose-Fermi mixtures in 3 dimensional optical lattices has been studied numerically within the DMFT-formalism[63] and analytically in a mean-field treatment[64] finding such phases as charge-density waves, superfluidity in either or both sectors, and supersolids. In 2 dimensional lattices the competition between s- and d-wave superfluidity and antiferromagnetic phases was investigated using the functional renormalization group[65].

In this work we restore some momentum fluctuations compared to the aforementioned DMFT study by studying mixtures in the Fermi liquid regime in a DCA framework in two dimensions and monitor the pairing susceptibilities. We assume that the bosons are deep in the superfluid phase which allows to find (exotic) pairing channels (unlike single-site DMFT) and the interplay with anti-ferromagnetic fluctuations but it rules out charge density wave order. We find that the

bosonic condensate can enhance both s- and d-wave pairing. Just as in conventional superconductors s-wave pairing is possible for weakly repulsive bare fermions. However, as the lattice effects and the bare Hubbard repulsion grow in importance, d-wave takes over and can be the dominant pairing channel. Atomic Bose-Fermi mixtures thus effectively display two different pairing mechanisms, relevant for superconductors.

II. MODEL

Our system is described by the fermionic action $S = S_f + S_{ret}$, with

$$S_f = \int_0^\beta d\tau \sum_{\langle i,j \rangle, \sigma} \bar{c}_i^\sigma(\tau) \left[\delta_{i,j} \left(\partial_\tau - \mu_f + n_0 U_{bf} \right) - t_f \right] c_j^\sigma(\tau)$$
$$+ U_{ff} \sum_i n_{i,\uparrow}^f(\tau) \, n_{i,\downarrow}^f(\tau) \qquad (1)$$
$$S_{ret} = -\frac{n_0 U_{bf}^2}{2} \iint_0^\beta d\tau_1 d\tau_2 \sum_{i,j} n_i^f(\tau_1) D_{ij}(\tau_1 - \tau_2) \, n_j^f(\tau_2).$$

It describes a fermionic Hubbard model with hopping amplitude t_f, on-site repulsion U_{ff} and chemical potential μ_f coupled to bosons deep in the condensed phase with condensate density n_0 via an on-site density-density coupling U_{bf}. The bosons are treated in the Bogoliubov approximation and subsequently integrated out, giving rise to the chemical potential shift $n_0 U_{bf}$ and the non-local retarded density-density action term S_{ret} with kernel

$$D(i-j,\tau) = \iint_{B.Z.} \frac{d^2k}{(2\pi)^d} e^{i\mathbf{k}(\mathbf{r}_i - \mathbf{r}_j)} \frac{e^{E_\mathbf{k}\tau} + e^{E_\mathbf{k}(\beta-\tau)}}{e^{\beta E_\mathbf{k}} - 1} \frac{|\bar{\varepsilon}_\mathbf{k}|}{E_\mathbf{k}} \qquad (2)$$

where $E_\mathbf{k} = \left[\bar{\varepsilon}_\mathbf{k}^2 + 2\bar{\varepsilon}_\mathbf{k} n_0 U_{bb} \right]^{1/2}$ is the dispersion of the Bogoliubov quasi-particles, $\bar{\varepsilon}_k = \varepsilon_\mathbf{k} - \varepsilon_\mathbf{0}$ the lattice dispersion of the bare bosons, shifted to be positive, and U_{bb} the repulsion between the bare bosons on the lattice. The chemical potential μ_b was fixed to give unit filling for the bosons (its density is unimportant in the superfluid regime). The explicit construction from the underlying Hamiltonian is performed in Appendix A. This treatment neglects any back-action of the fermions on the bosons, in particular, bosonic charge order is excluded, which might be mediated from the fermionic sector by the density-density coupling between bosons and fermions. However, for fast bosons (amounting to $t_b > t_f$) which we consider, charge-density ordering was found to be suppressed and superconductivity to be favored in DMFT[63].

In the instantaneous limit, $i.e.$, the case of a very high bosonic speed of sound compared to the Fermi velocity as it can be made in the NaK system[3], this simplifies to $D_{inst}(\mathbf{k}) = \frac{1}{n_0 U_{bb}} c(\mathbf{k}) = \frac{1}{n_0 U_{bb}} \left\{ 1 + \xi^2 \left[4 - \cos(k_x) - \cos(k_y) \right] \right\}^{-1}$, with

$\xi = \sqrt{t_b/(2U_{bb})}$ as obtained in[65]. The induced on-site interaction is given by $W = \frac{U_{bf}^2}{U_{bb}} \sum_\mathbf{k} c(\mathbf{k})$, thus scaling as $V = U_{bf}^2/U_{bb}$. The bosonic dispersion E_k can only have an influence on the fermionic system if ξ is comparable to the lattice spacing, which is satisfied for NaK.

III. METHODOLOGY

To numerically study the action Eq. (1) we use the dynamical cluster approximation (DCA)[66–68], which maps the many-body problem onto a self-consistently embedded cluster impurity problem. Its action $S = S_0 + S_{int}$ reads

$$S_0 = \int_0^\beta d\tau \sum_{i,j,\sigma} \bar{c}_i^\sigma(\tau_1) \mathcal{G}_{\sigma,i,j}^{-1}(\tau_1 - \tau_2) c_j^\sigma(\tau_2) \qquad (3)$$
$$S_{int} = U_{ff} \sum_i n_{i,\uparrow}^f(\tau) \, n_{i,\downarrow}^f(\tau) + S_{ret} \qquad (4)$$

Here, the sums run over the cluster degrees of freedom, $\mathcal{G}$ is the unknown cluster-excluded Green's function of the impurity problem which has to be determined self-consistently. The local Hubbard interaction U_{ff} remains unaffected by the DCA mapping, but the non-local induced interaction is coarse-grained, $i.e.$, D_{ij} in S_{ret} is replaced by $\bar{D}_{ij}$, which is the Cluster-Fourier transform of the coarse-grained interaction kernel $D(i - j)$.

To solve the impurity problem, we use a generalized weak-coupling solver[69,70] to include the non-local phononic degrees of freedom similar as in Ref.[71]. We are limited to 2×2 clusters because of the sign problem, which also occurs at half filling because the induced interactions, $\bar{D}_{i,j}(\tau)$ (Eq. 2), do not have a definite sign. Results of the average sign for characteristic values of the parameters and temperatures used in our simulations are shown in Appendix B. Unfortunately, 2×2 clusters are known to overestimate the d-wave transition temperature and to strongly suppress antiferromagnetic phases[68,72]. Bigger clusters are highly desired to take the Kosterlitz-Thouless transitions properly into account, but are out of reach.

To obtain transitions to a superconducting state we need to consider the two-particle Green's function for opposite spin pairing in the particle-particle channel

$$\chi(q,k,k') = \int_0^\beta \int_0^\beta \int_0^\beta \int_0^\beta d\tau_1 d\tau_2 d\tau_3 d\tau_4 \qquad (5)$$
$$\times e^{i[(\omega_n+\nu)\tau_1 - \omega_n\tau_2 + \omega_{n'}\tau_3 - (\omega_{n'}+\nu)\tau_4]} \langle T_\tau P(\cdot) \rangle$$
$$P(\cdot) = c_{\mathbf{k}+\mathbf{q},\sigma}^\dagger(\tau_1) \, c_{-\mathbf{k},-\sigma}^\dagger(\tau_2) \, c_{-\mathbf{k}',-\sigma}(\tau_3) \, c_{\mathbf{k}'+\mathbf{q},\sigma}(\tau_4)$$

where we adopt the notation $k = (\mathbf{k}, i\omega_n)$, $k' = (\mathbf{k}', i\omega_{n'})$ and $q = (\mathbf{q}, i\nu_n)$[73]. For transitions to states of lower symmetry than the lattice, the Green's function needs to be projected according to

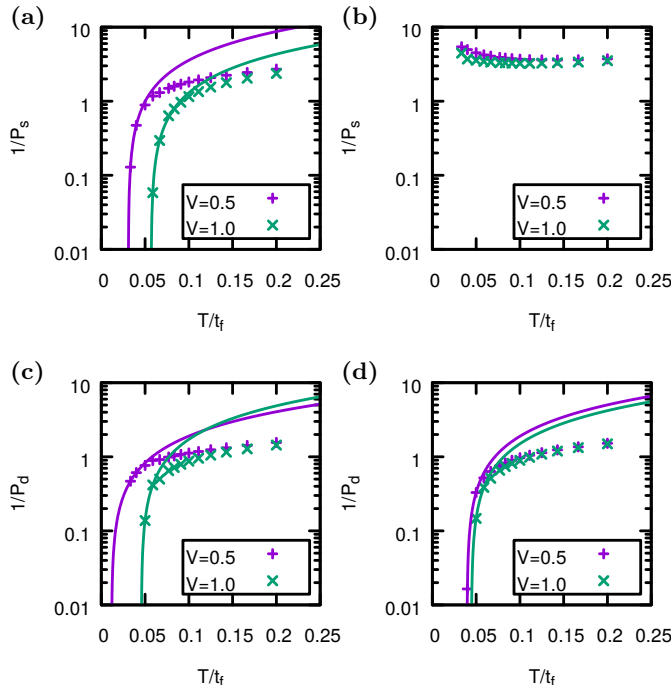$$\Pi_{g,g}(q,k,k') = g(\mathbf{k})\chi(q,k,k')g(\mathbf{k}') \qquad (6)$$

Figure 1. Inverse pairing field susceptibility $1/P_g$ on a logarithmic scale for $g = s(d)$-wave symmetry at the top (bottom) at fixed $U_{\mathrm{ff}} = 0(1)$ at the left (right) and fermionic half filling as a function of temperature for different coupling strength U_{bf} to the bosons corresponding to $V = 0.5, 1.0$ for the bosonic parameters $U_{\mathrm{bb}}/t_{\mathrm{f}} = 5$ and $t_{\mathrm{b}}/t_{\mathrm{f}} = 10$. The vanishing of $1/P_g$ signals the transition to a superconducting state of the corresponding symmetry. The solid lines are linear fits to the lowest temperature points and are used to derive T_c.

where $g(\mathbf{k})$ is the form-factor for the corresponding symmetry. The pairing susceptibility is then given by

$$P_g(q, T) = \frac{T^2}{N_c^2} \sum_{K,K'} \overline{\Pi}_{g,g}(q, K, K') \,. \tag{7}$$

where $\overline{\Pi}$ is the coarse-grained version of $\Pi_{g,g}$ obtained by inverting the coarse-grained Bethe-Salpeter equation as described in[67]. The calculation of the corresponding quantity for pairing in the particle-hole channel, relevant for transitions to an antiferromagnetic state, is similar and explained in detail in[68].

IV. RESULTS

We now turn to the investigation of the fermionic instabilities, which is reflected in the behavior of susceptibilities in the particle-hole and particle-particle channels, specifically the antiferromagnetic susceptibility χ_{AF} at momentum transfer $q = ((\pi, \pi), 0)$ and the pairing field susceptibility P_g as defined in Eq. (7) for the dominant momentum transfer $q = (\mathbf{0}, 0)$ in the case
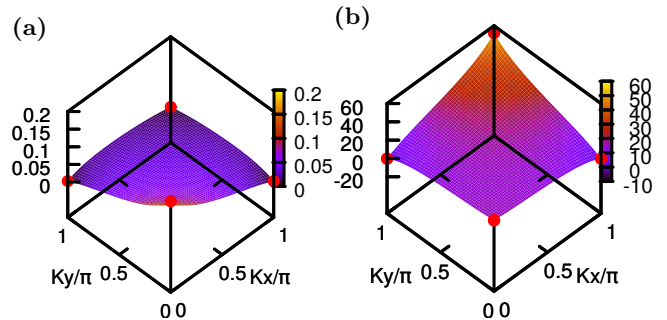

Figure 2. Pairing vertex in the particle-particle channel $\Gamma^{PP}(\mathbf{K} - \mathbf{K}')$ as a function of the relative momentum for $U_{\mathrm{ff}}/t_{\mathrm{f}} = 0.2$, $V/t_{\mathrm{f}} = 2$ in (a) where s-wave pairing dominates showing a peak at $\mathbf{K} - \mathbf{K}' = (0, 0)$ and for $U_{\mathrm{ff}}/t_{\mathrm{f}} = 5$, $V/t_{\mathrm{f}} = 1$ in (b) where d-wave pairing dominates displaying a clear peak at $\mathbf{K} - \mathbf{K}' = (\pi, \pi)$.

of the s-, extended s-, p- and d-wave symmetry[67,72]. The divergence of the pairing field signals the phase transition to the state of the corresponding symmetry. To obtain the respective transition temperature we fit a linear function to the pairing fields in the low-temperature region as is appropriate for the mean-field nature of DCA close to T_c[68,72]. At half filling, we only found transitions to s- and d-wave, as well as strong antiferromagnetic correlations, whose competition is the focus of what follows.

The $s(d)$-wave pairing fields with the linear fits are shown in the upper (lower) panel of Fig. (1). In the free model ($U_{\mathrm{ff}} = U_{\mathrm{bf}} = 0$) there is no pairing in either channel. When increasing U_{bf} (but keeping $U_{\mathrm{ff}} = 0$), competing s- and d-wave instabilities develop as seen in the left panel. For $U_{\mathrm{bf}}/t_{\mathrm{f}} = 1.58$, i.e., $V/t_{\mathrm{f}} = 0.5$, we observe that the extrapolated s-wave transition temperature is higher than the d-wave one and s-wave pairing is thus the dominant channel. For weak V the mechanism for induced s-wave superconductivity is the same as in BCS theory. Upon increasing V, the s-wave gap becomes stronger and we enter the regime where superconductors are routinely described by the Migdal-Eliashberg theory[58,74–79]. The momentum dependence of the bosonic dispersion E_k is here unimportant but retardation effects do matter in general. A selfconsistent treatment of the bosons (e.g., via a damping term) is left for future work.

Upon increasing U_{ff} s-wave-pairing is suppressed and d-wave is the dominant instability as seen in the right panel for $U_{\mathrm{ff}}/t_{\mathrm{f}} = 1$ where no s-wave instability is found for the range of V shown. This is easily understood in the instantaneous limit where W scales with $V = U_{\mathrm{bf}}^2/U_{\mathrm{bb}}$ and for $|W| < |U_{\mathrm{ff}}|$ no s-wave pairing is possible.

The competition between s- and d-wave pairing is also clearly reflected in the momentum structure of the pairing vertex shown in Fig. (2) in (a) for a situation where s-wave dominates and in (b) where d-wave is dominant.
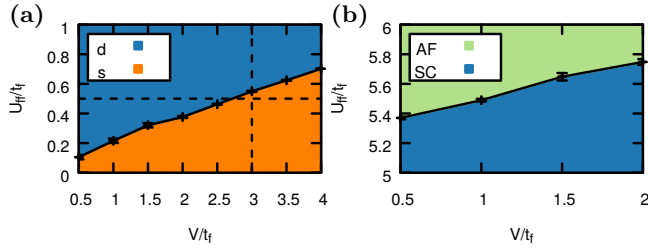
Figure 3. (a) Phase diagram based on the transition temperatures obtained from the linear extrapolation of the inverse pairing field susceptibilities P_g for the competing instabilities towards s- and d-wave pairing for bosonic parameters $U_{\mathrm{bb}}/t_{\mathrm{f}} = 5$ and $t_{\mathrm{b}}/t_{\mathrm{f}} = 10$. The phase transition line corresponds to the critical coupling U_{ff}^c where the computed transition temperatures for the respective phases cross. The dashed lines correspond to the cuts along which the transition temperatures are shown in Fig. 4. (b) Phase diagram focusing on the transition between the cluster antiferromagnetic instability ('AF') and the superconducting phase ('SC').
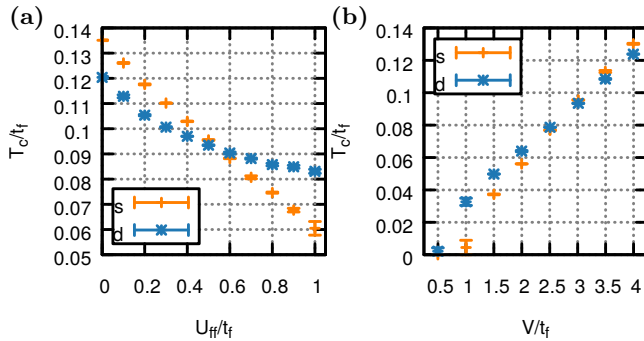

Figure 4. Critical temperature T_c for s- and d-wave pairing as a function of U_{ff} at fixed $V/t_{\mathrm{f}} = 3$ in (a) and as a function of V at fixed $U_{\mathrm{ff}}/t_{\mathrm{f}} = 0.5$ in (b).

In the case of s-wave pairing the vertex peaks at a zero momentum transfer leading to a homogeneous real space structure whereas for d-wave a strong peak develops for a momentum transfer $\mathbf{K} - \mathbf{K}' = (\pi, \pi)$ leading to oscillatory behaviour in real space.

Based on the extrapolated transition temperatures we obtain the phase-diagram in Fig (3)(a). For the bosonic parameters $U_{\mathrm{bb}}/t_{\mathrm{f}} = 5$ and $t_{\mathrm{b}}/t_{\mathrm{f}} = 10$ we have that $W \approx 0.25V$ and we expect s-wave pairing to become relevant around $V \approx 4W \sim 4|U_{\mathrm{ff}}|$. Indeed, on increasing U_{bf} we first observe increasing transition temperatures for d-wave pairing up to the regime $|W| \gtrsim |U_{\mathrm{ff}}|$.

The critical temperatures for s- and d-wave pairing along cuts in the phase-diagram are shown in Fig (4). As the 2×2 cluster represents the mean-field result for d-wave, underestimating the fluctuations and consequently overestimating the d-wave transition temperatures, we expect the transition line to shift in favor of s-wave in those regions in which the s-wave transition
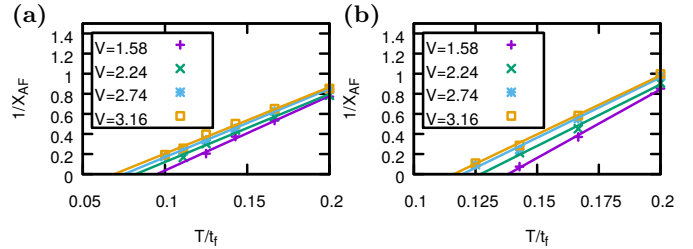

Figure 5. Inverse pairing field susceptibility $1/\chi_{AF}$ as a function of temperature T/t_f at fixed $U_{\mathrm{ff}} = 5.2(5.8)$ to the left (right) and fermionic half filling for different coupling strength U_{bf} to the bosons corresponding to $V = 0.5, 1.0, 1.5, 2.0$ for the bosonic parameters $U_{\mathrm{bb}}/t_{\mathrm{f}} = 5$ and $t_{\mathrm{b}}/t_{\mathrm{f}} = 10$. The vanishing of $1/P_{AF}$ signals the transition to an AFM state. The solid lines are linear fits to the lowest temperature points and are used to derive T_c.

temperature is finite, *i.e.*, qualitatively those for which the effective induced interaction W is stronger than the repulsion given by U_{ff}.

Next we consider the instability towards an antiferromagnetic state. In the thermodynamical limit antiferromagnetism is allowed at zero temperature only but in selfconsistent cluster approaches such as DCA it can be found at finite temperature as well, rather accurately reproducing correlations at short distances but missing their fluctuations at long distances.

The spin susceptibility $\chi_{AF}(T)$, corresponding to an instability in the spin sector of the particle-hole channel, is shown in Fig. 5 for $U_{\mathrm{ff}} = 5.2, 5.8$ and for different values of the strength of the induced interaction $V = 0.5, 1.0, 1.5, 2.0$. To obtain the Neel temperature which corresponds to the divergence of $\chi_{AF}(T)$ a linear function to the inverse spin susceptibility in the low-temperature region is used as explained above.

Based on the extrapolated transition temperatures for the divergence of the antiferromagnetic susceptibility χ_{AF}, we obtain a transition to an AFM state as shown in the corresponding phase diagram in Fig (3)(b). Again a stronger Fermi-Bose coupling V tends to stabilise the d-wave state, in turn shifting the transition to the AFM state to higher values of U_{ff}. The transition to the AFM state appears at considerably higher U_{ff} than in[65], because the 2×2 cluster is known to strongly suppress antiferromagnetism[68,72], thus favoring the superconducting state.

From these observations it emerges that increasing V enhances both s- and d-wave (with s-wave being dominant for nearly-free fermions). Increasing U_{ff} increases the spin density wave fluctuations and suppresses s-wave pairing, as a result of which d- can become dominant over an extended regime in parameter space. This suggests that T_c for d-wave can be increased by increasing both V and U_{ff} and staying near the line where s-wave becomes subdominant compared to d-wave. In the static mean-field study of Ref.[3] the highest T_c for a NaK mixture was found at $\xi = 0.6$. For those parameters we find

a maximal $T_c/t = 0.17$. Whereas Migdal-Eliashberg theories usually do not have a built-in mechanism that puts a limit on T_c, the gain stops here when U_{bf} is too large compared to U_{ff} and U_{bb} causing a mechanical instability towards phase-separation[25,27].

V. CONCLUSIONS

In this work we studied the antiferromagnetic und superconducting instabilities of Bose-Fermi-Mixtures in the limit where the bosons can be treated within the Bogoliubov approximation. We used a weak coupling Monte-Carlo cluster solver within the DCA-framework allowing us to distinguish between s- and d-wave pairing in the fermionic sector. The dominant pairing mechanism is determined by the relative sizes of the repulsive fermi-fermi interaction U_{ff} and the interactions induced by the bosons scaling with $V = U_{bf}^2/U_{bb}$ leading to the phase diagram shown in Fig (3)(a). In particular, we find that d-wave superconductivity can be stabilized by the presence of bosonic particles. This extends the results of a recent DMFT study[63] which found phases in which both bosons and fermions are superfluid, but could not determine the symmetry of the superfluid state. In addition, for strong Fermi-Fermi interaction, we observe a transition to an antiferromagnetic state suppressing the superconducting pairing as seen in Fig (3)(b), consistent with a previous study based on the functional renormalization group[65]. Our approach holds whenever the bosonic speed of sound c is larger than the Fermi velocity v_F. We checked that for $c/v_F = 2$ the phase diagram looks similar but with stronger retardation effects. Our work can straightforwardly be extended to doped systems, allowing to address the strange metal physics and where also $p-$wave phases are predicted. The mechanisms discussed here are equally valid in 3d where T_c for d-wave could well be much higher than in 2d.

Appendix A: Derivation of the effective action

In this appendix we explicitly discuss the construction of the effective action in Eq. 1. Starting from the Hamil-

tonian of Bose-Fermi-Mixtures on a 2D square lattice

$$
\begin{aligned}
H =& H_f + H_b + H_{bf} \\
=& -t_f \sum_{<i,j>,\sigma} c_{i,\sigma}^\dagger c_{j,\sigma} - \mu_f \sum_{i,\sigma} n_{i,\sigma}^f + U_{ff} \sum_i n_{i,\uparrow}^f n_{i,\downarrow}^f \\
& -t_b \sum_{<i,j>} b_i^\dagger b_j - \mu_b \sum n_i^b + \frac{U_{bb}}{2} \sum n_i^b(n_i^b - 1) \\
& + U_{bf} \sum_{i,\sigma} n_i^b n_{i,\sigma}^f
\end{aligned}
\tag{A1}
$$

where $c_i^\dagger$ ($b_i^\dagger$) are fermionic (bosonic) creation operators at site i, $n_i^{f(b)}$ the corresponding densities, $t_{f(b)}$ describes the hopping of a fermion (boson) from site i to site j, $\mu_{f(b)}$ is the chemical potential for fermions (bosons), $U_{ff(bb)}$ is the on-site repulsion of fermions (bosons) and U_{bf} the on-site interaction between bosons and fermions. The model is the sum of a Fermi-Hubbard model (first line) the Bose-Hubbard model (second line) and a density-density interaction between bosons and fermions (third line). In the following we will treat the bosons within the Bogoliubov approximation allowing us to integrate them out in favour of a retarded density-density interaction between fermions.

In the Bogoliubov approximation the bosonic Hamiltonian H_b takes the form $H_b \approx \sum_\mathbf{k} E_\mathbf{k} \alpha_\mathbf{k}^\dagger \alpha_\mathbf{k}$ in terms of the Bogoliubov quasi-particles defined by $b_\mathbf{k} = u_\mathbf{k} \alpha_\mathbf{k} - v_\mathbf{k} \alpha_{-\mathbf{k}}^\dagger$ and $b_\mathbf{k}^\dagger = u_\mathbf{k} \alpha_\mathbf{k}^\dagger - v_\mathbf{k} \alpha_{-\mathbf{k}}$ respectively. As usual the coefficients are given by $u_\mathbf{k} = \cosh\phi_\mathbf{k}$ and $v_\mathbf{k} = \sinh\phi_\mathbf{k}$ where $\tanh 2\phi_\mathbf{k} = n_0 U_{bb}/(\bar{\varepsilon}_\mathbf{k} + n_0 U_{bb})$. The Bogoliubov spectrum is given by $E_\mathbf{k} = \left[\bar{\varepsilon}_\mathbf{k}^2 + 2\bar{\varepsilon}_\mathbf{k} n_0 U_{bb}\right]^{1/2}$ with $\bar{\varepsilon}_\mathbf{k} = \varepsilon_\mathbf{k} - \varepsilon_\mathbf{0}$, the lattice dispersion of non-interacting bosons shifted to be positive. We emphasize that this treatment neglects any backaction of the fermionic sector on the bosons, in particular we assume that the bosons do not charge order, which limits our approach to the case of fast bosons.

Rewriting the coupling term H_{bf} in momentum space we obtain

$$
H_{bf} = \frac{1}{N_s} \sum_{i,\mathbf{k}_1,\mathbf{k}_2} e^{-i(\mathbf{k}_1-\mathbf{k}_2)\mathbf{r}_i} b_{\mathbf{k}_1}^\dagger b_{\mathbf{k}_2} n_i^f
\tag{A2}
$$

$$
= \frac{N_0}{N_s} \sum_i n_i^f + \frac{\sqrt{N_0}}{N_s} \sideset{}{'}\sum_{i,k} \left(e^{ikr_i} b_\mathbf{k} + e^{-ikr_i} b_\mathbf{k}^\dagger \right) n_i^f
$$

$$
+ \frac{1}{N_s} \sideset{}{'}\sum_{i,\mathbf{k}_1,\mathbf{k}_2} e^{-i(\mathbf{k}_1-\mathbf{k}_2)r_i} b_{\mathbf{k}_1}^\dagger b_{\mathbf{k}_2} n_i^f
\tag{A3}
$$

where N_0 is the macroscopic number of bosonic atoms in the condensate, N_s is the number of sites in the lattice and the primed sum indicates that the $k=0$ terms should be omitted. In the following we will neglect the last term as it is suppressed by a power of $\sqrt{N_0}$ compared to the second term. The first term corresponds to the shift in the fermionic chemical potential present in

Eq. 1 whereas the second term represents the linear coupling of bosons to the fermions that will be integrated out.

Next, we reexpress the second term in the Bogoliubov boson operators to obtain

$$\sum_{i\mathbf{k}}' \left(e^{i\mathbf{kr}_i} b_{\mathbf{k}} + e^{-i\mathbf{kr}_i} b_{\mathbf{k}}^{\dagger} \right) n_i^f$$
$$= \sum_{i,\mathbf{k}}' \left(\alpha_{\mathbf{k}} \left[u_{\mathbf{k}} - v_{-\mathbf{k}} \right] e^{i\mathbf{kr}_i} + \alpha_{\mathbf{k}}^{\dagger} \left[u_{\mathbf{k}} - v_{-\mathbf{k}} \right] e^{-i\mathbf{kr}_i} \right) n_i^f .$$
(A4)

which clearly shows that the Bogoliubov bosons couple linearly to the fermionic density with momentum dependent couplings.

Employing coherent states for both the bosons and fermions the action reads as $S = S_{\mathrm{f}} + S_{\mathrm{bog}} + S_{\mathrm{bf}}$ where the fermionic action S_f has already been defined in Eq. 1 and

$$S_{\mathrm{bog}} = \int_0^{\beta} d\tau \sum_{\mathbf{k}} \bar{\alpha}_{\mathbf{k}}(\tau) \left[E_{\mathbf{k}} + \frac{\partial}{\partial \tau} \right] \alpha_{\mathbf{k}}(\tau)$$
(A5)

$$S_{\mathrm{bf}} = \sqrt{n_0}\, U_{\mathrm{bf}} \int_0^{\beta} d\tau \, \frac{1}{\sqrt{N_s}} \sum_{i,\mathbf{k}} \Big(\alpha_{\mathbf{k}}(\tau) \left[u_{\mathbf{k}} - v_{-\mathbf{k}} \right] e^{i\mathbf{kr}_i}$$
$$+ \bar{\alpha}_{\mathbf{k}}(\tau) \left[u_{\mathbf{k}} - v_{-\mathbf{k}} \right] e^{-i\mathbf{kr}_i} \Big) n_i^f(\tau)$$
(A6)

Finally, integration over the quadratic bosonic Bogoliubov action yields the non-local, retarded density-density interaction, i.e. $e^{-S_{ret}} = \int d(\bar{\alpha}, \alpha) e^{-S_{\mathrm{bog}} - S_{\mathrm{bf}}}$ with

$$S_{\mathrm{ret}} = -\frac{n_0\, U_{\mathrm{bf}}^2}{2} \iint_0^{\beta} d\tau_1 d\tau_2 \sum_{i,j} n_i^f(\tau_1)\, D_{ij}(\tau_1 - \tau_2)\, n_j^f(\tau_2)$$
(A7)

which combined with S_f gives the total action $S = S_f + S_{\mathrm{ret}}$ of the effective model in Eq. 1 and the kernel D_{ij} has been defined in Eq. 2.

Appendix B: Discussion of the sign problem

As we are at half-filling the simulations are sign-free for $V = 0$. However, as discussed in the main text the induced interactions lead to a sign-problem. The average sign of the simulations is shown in Fig. 6 in each panel at a fixed value of U_{ff} for different values of $V = U_{\mathrm{bf}}^2/U_{\mathrm{bb}}$.

We only observe a very weak dependence of the sign on the fermi-fermi interaction U_{ff} as expected from the sign free character for $V = 0$. In all cases the sign is exponentially decreasing as a function of β with a decay rate that increases as V is increased and the induced interactions become more important. This exponential dependence on the temperatures limits the lowest temperatures we can access in the simulations. Moreover,
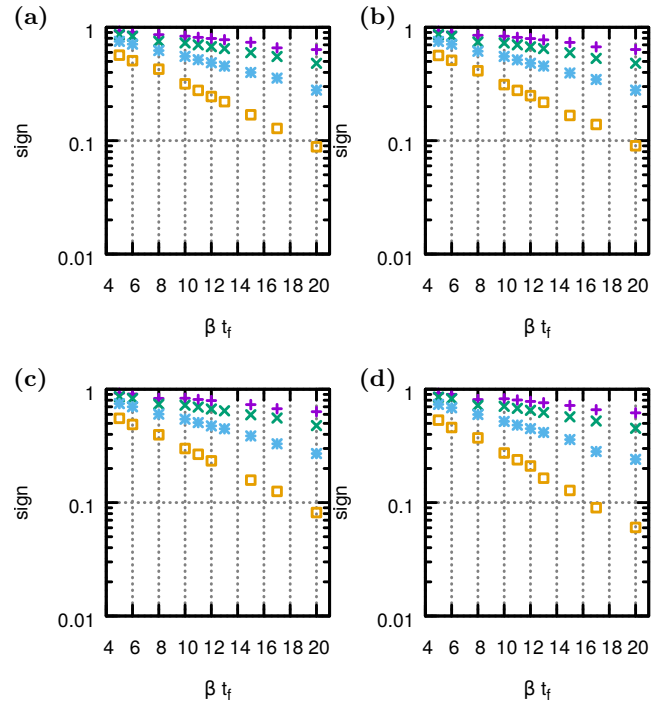

Figure 6. Average sign of the Monte-Carlo simulations as a function of β for $U_{\mathrm{ff}}/t_f = 1, 2, 3, 4$ in panels (a)-(d), in each case for $V/t_f = 0.5, 1.0, 2.0, 4.0$ from top to bottom.

the strong dependence on the induced interactions limits the maximally accessible V and ultimately the extension to bigger clusters where the number of interaction terms proliferates.

* tb494@cam.ac.uk
[1] Immanuel Bloch and Wilhelm Zwerger, "Many-body physics with ultracold gases," Rev. Mod. Phys. **80**, 885–964 (2008).
[2] W. Ketterle and M. W. Zwierlein, "Making, probing and understanding ultracold Fermi gases," Nuovo Cimento

Rivista Serie **31**, 247–422 (2008), arXiv:0801.2500 [cond-mat.other].
[3] D.-W. Wang, M. D. Lukin, and E. Demler, "Engineering superfluidity in bose-fermi mixtures of ultracold atoms," Phys. Rev. A **72**, 051604 (2005).
[4] D. J. Scalapino, E. Loh, and J. E. Hirsch, "d-wave pairing

near a spin-density-wave instability," Phys. Rev. B **34**, 8190–8192 (1986).

[5] Ar. Abanov, A. V. Chubukov, and A. M. Finkel'stein, "Coherent vs . incoherent pairing in 2D systems near magnetic instability," EPL (Europhysics Letters) **54**, 488 (2001).

[6] Ar. Abanov, Andrey V. Chubukov, and J. Schmalian, "Quantum-critical theory of the spin-fermion model and its application to cuprates: Normal state analysis," Advances in Physics **52**, 119–218 (2003), http://dx.doi.org/10.1080/0001873021000057123.

[7] Yuxuan Wang and Andrey V. Chubukov, "Superconductivity at the onset of spin-density-wave order in a metal," Phys. Rev. Lett. **110**, 127001 (2013).

[8] Max A Metlitski and Subir Sachdev, "Instabilities near the onset of spin density wave order in metals," New Journal of Physics **12**, 105007 (2010).

[9] Max A. Metlitski and Subir Sachdev, "Quantum phase transitions of metals in two spatial dimensions. ii. spin density wave order," Phys. Rev. B **82**, 075128 (2010).

[10] Erez Berg, Max A. Metlitski, and Subir Sachdev, "Sign-problem–free quantum monte carlo of the onset of antiferromagnetism in metals," Science **338**, 1606–1609 (2012), http://www.sciencemag.org/content/338/6114/1606.full.pdf.

[11] Eun Gook Moon and Subir Sachdev, "Competition between spin density wave order and superconductivity in the underdoped cuprates," Phys. Rev. B **80**, 035117 (2009).

[12] Subir Sachdev, Max A Metlitski, and Matthias Punk, "Antiferromagnetism in metals: from the cuprate superconductors to the heavy fermion materials," Journal of Physics: Condensed Matter **24**, 294205 (2012).

[13] D. J. Scalapino, "A common thread: The pairing interaction for unconventional superconductors," Rev. Mod. Phys. **84**, 1383–1417 (2012).

[14] Hui Zhai, Fa Wang, and Dung-Hai Lee, "Antiferromagnetically driven electronic correlations in iron pnictides and cuprates," Phys. Rev. B **80**, 064517 (2009).

[15] Eun Gook Moon and Subir Sachdev, "Quantum critical point shifts under superconductivity: Pnictides and cuprates," Phys. Rev. B **82**, 104516 (2010).

[16] Kazuhiko Kuroki, Seiichiro Onari, Ryotaro Arita, Hidetomo Usui, Yukio Tanaka, Hiroshi Kontani, and Hideo Aoki, "Unconventional pairing originating from the disconnected fermi surfaces of superconducting lafeaso$_{1-x}$f$_x$," Phys. Rev. Lett. **101**, 087004 (2008).

[17] I. I. Mazin, D. J. Singh, M. D. Johannes, and M. H. Du, "Unconventional superconductivity with a sign reversal in the order parameter of lafeaso$_{1-x}$f$_x$," Phys. Rev. Lett. **101**, 057003 (2008).

[18] S Graser, T A Maier, P J Hirschfeld, and D J Scalapino, "Near-degeneracy of several pairing channels in multiorbital models for the Fe pnictides," New Journal of Physics **11**, 025016 (2009).

[19] Saurabh Maiti and Andrey V. Chubukov, "Renormalization group flow, competing phases, and the structure of superconducting gap in multiband models of iron-based superconductors," Phys. Rev. B **82**, 214515 (2010).

[20] Paglione Johnpierre and Greene Richard L., "High-temperature superconductivity in iron-based materials," Nat Phys **6**, 645–658 (2010), 10.1038/nphys1759.

[21] David C. Johnston, "The puzzle of high temperature superconductivity in layered iron pnictides and chalcogenides," Advances in Physics **59**, 803–1061 (2010), http://dx.doi.org/10.1080/00018732.2010.513480.

[22] Gegenwart Philipp, Si Qimiao, and Steglich Frank, "Quantum criticality in heavy-fermion metals," Nat Phys **4**, 186–197 (2008), 10.1038/nphys892.

[23] Sunil Nair, O. Stockert, U. Witte, M. Nicklas, R. Schedler, K. Kiefer, J. D. Thompson, A. D. Bianchi, Z. Fisk, S. Wirth, and F. Steglich, "Magnetism and superconductivity driven by identical 4f states in a heavy-fermion metal," Proceedings of the National Academy of Sciences **107**, 9537–9540 (2010), http://www.pnas.org/content/107/21/9537.full.pdf.

[24] Z. Hadzibabic, C. A. Stan, K. Dieckmann, S. Gupta, M. W. Zwierlein, A. Görlitz, and W. Ketterle, "Two-species mixture of quantum degenerate bose and fermi gases," Phys. Rev. Lett. **88**, 160401 (2002).

[25] H. P. Büchler and G. Blatter, "Supersolid versus phase separation in atomic bose-fermi mixtures," Phys. Rev. Lett. **91**, 130404 (2003).

[26] M. Lewenstein, L. Santos, M. A. Baranov, and H. Fehrmann, "Atomic bose-fermi mixtures in an optical lattice," Phys. Rev. Lett. **92**, 050401 (2004).

[27] H. P. Büchler and G. Blatter, "Phase separation of atomic bose-fermi mixtures in an optical lattice," Phys. Rev. A **69**, 063603 (2004).

[28] M. Cramer, J. Eisert, and F. Illuminati, "Inhomogeneous atomic bose-fermi mixtures in cubic lattices," Phys. Rev. Lett. **93**, 190405 (2004).

[29] Robert Roth and Keith Burnett, "Quantum phases of atomic boson-fermion mixtures in optical lattices," Phys. Rev. A **69**, 021601 (2004).

[30] C. Silber, S. Günther, C. Marzok, B. Deh, Ph. W. Courteille, and C. Zimmermann, "Quantum-degenerate mixture of fermionic lithium and bosonic rubidium gases," Phys. Rev. Lett. **95**, 170408 (2005).

[31] C. Ospelkaus, S. Ospelkaus, L. Humbert, P. Ernst, K. Sengstock, and K. Bongs, "Ultracold heteronuclear molecules in a 3d optical lattice," Phys. Rev. Lett. **97**, 120402 (2006).

[32] S. Ospelkaus, C. Ospelkaus, L. Humbert, K. Sengstock, and K. Bongs, "Tuning of heteronuclear interactions in a degenerate fermi-bose mixture," Phys. Rev. Lett. **97**, 120403 (2006).

[33] Kenneth Günter, Thilo Stöferle, Henning Moritz, Michael Köhl, and Tilman Esslinger, "Bose-fermi mixtures in a three-dimensional optical lattice," Physical Review Letters **96** (2006), 10.1103/physrevlett.96.180402.

[34] Stephen Powell, Subir Sachdev, and Hans Peter Büchler, "Depletion of the bose-einstein condensate in bose-fermi mixtures," Phys. Rev. B **72**, 024534 (2005).

[35] K.-K. Ni, S. Ospelkaus, M. H. G. de Miranda, A. Pe'er, B. Neyenhuis, J. J. Zirbel, S. Kotochigova, P. S. Julienne, D. S. Jin, and J. Ye, "A high phase-space-density gas of polar molecules," Science **322**, 231–235 (2008), http://www.sciencemag.org/content/322/5899/231.full.pdf.

[36] Th. Best, S. Will, U. Schneider, L. Hackermüller, D. van Oosten, I. Bloch, and D.-S. Lühmann, "Role of interactions in rb87-K40 Bose-fermi mixtures in a 3D optical lattice," Physical Review Letters **102** (2009), 10.1103/physrevlett.102.030408.

[37] Lode Pollet, Matthias Troyer, Kris Van Houcke, and Stefan M. A. Rombouts, "Phase diagram of bose-fermi mixtures in one-dimensional optical lattices," Phys. Rev. Lett. **96**, 190402 (2006).

[38] Lode Pollet, Corinna Kollath, Ulrich Schollwöck, and

Matthias Troyer, "Mixture of bosonic and spin-polarized fermionic atoms in an optical lattice," Phys. Rev. A **77**, 023608 (2008).

[39] Francesca M. Marchetti, Charles J. M. Mathy, David A. Huse, and Meera M. Parish, "Phase separation and collapse in bose-fermi mixtures with a feshbach resonance," Phys. Rev. B **78**, 134517 (2008).

[40] Elisa Fratini and Pierbiagio Pieri, "Pairing and condensation in a resonant bose-fermi mixture," Phys. Rev. A **81**, 051605 (2010).

[41] Anders H. Hansen, Alexander Khramov, William H. Dowd, Alan O. Jamison, Vladyslav V. Ivanov, and Subhadeep Gupta, "Quantum degenerate mixture of ytterbium and lithium atoms," Phys. Rev. A **84**, 011606 (2011).

[42] Hideaki Hara, Yosuke Takasu, Yoshifumi Yamaoka, John M. Doyle, and Yoshiro Takahashi, "Quantum degenerate mixtures of alkali and alkaline-earth-like atoms," Phys. Rev. Lett. **106**, 205304 (2011).

[43] Zeng-Qiang Yu, Shizhong Zhang, and Hui Zhai, "Stability condition of a strongly interacting boson-fermion mixture across an interspecies feshbach resonance," Phys. Rev. A **83**, 041603 (2011).

[44] G. Bertaina, E. Fratini, S. Giorgini, and P. Pieri, "Quantum monte carlo study of a resonant bose-fermi mixture," Phys. Rev. Lett. **110**, 115303 (2013).

[45] Andrea Guidini, Gianluca Bertaina, Davide Emilio Galli, and Pierbiagio Pieri, "Condensed phase of bose-fermi mixtures with a pairing interaction," Phys. Rev. A **91**, 023603 (2015).

[46] I. Ferrier-Barbut, M. Delehaye, S. Laurent, A. T. Grier, M. Pierce, B. S. Rem, F. Chevy, and C. Salomon, "A mixture of bose and fermi superfluids," Science **345**, 1035–1038 (2014), http://www.sciencemag.org/content/345/6200/1035.full.pdf.

[47] Wei Zheng and Hui Zhai, "Quasiparticle lifetime in a mixture of bose and fermi superfluids," Phys. Rev. Lett. **113**, 265304 (2014).

[48] J. J. Kinnunen and G. M. Bruun, "Induced interactions in a superfluid bose-fermi mixture," Phys. Rev. A **91**, 041605 (2015).

[49] Cheng-Hsun Wu, Ibon Santiago, Jee Woo Park, Peyman Ahmadi, and Martin W. Zwierlein, "Strongly interacting isotopic bose-fermi mixture immersed in a fermi sea," Phys. Rev. A **84**, 011601 (2011).

[50] Jee Woo Park, Cheng-Hsun Wu, Ibon Santiago, Tobias G. Tiecke, Sebastian Will, Peyman Ahmadi, and Martin W. Zwierlein, "Quantum degenerate Bose-fermi mixture of chemically different atomic species with widely tunable interactions," Phys. Rev. A **85** (2012), 10.1103/physreva.85.051602.

[51] Jee Woo Park, Sebastian A. Will, and Martin W. Zwierlein, "Ultracold dipolar gas of fermionic $^{23}Na^{40}K$ molecules in their absolute ground state," Phys. Rev. Lett. **114**, 205302 (2015).

[52] M. Bijlsma, B. Heringa, and H. Stoof, "Phonon exchange in dilute fermi-Bose mixtures: Tailoring the fermi-fermi interaction," Phys. Rev. A **61** (2000), 10.1103/physreva.61.053601.

[53] H. Heiselberg, C. Pethick, H. Smith, and L. Viverit, "Influence of induced interactions on the superfluid transition in dilute fermi gases," Physical Review Letters **85**, 2418–2421 (2000).

[54] Giovanni Modugno, Giacomo Roati, Francesco Riboli, Francesca Ferlaino, Robert J. Brecha, and Massimo Inguscio, "Collapse of a degenerate fermi gas," Science **297**, 2240–2243 (2002), http://www.sciencemag.org/content/297/5590/2240.full.pdf.

[55] L. Viverit and S. Giorgini, "Ground-state properties of a dilute Bose-fermi mixture," Phys. Rev. A **66** (2002), 10.1103/physreva.66.063604.

[56] L. Viverit, "Boson-induced s-wave pairing in dilute boson-fermion mixtures," Phys. Rev. A **66**, 023605 (2002).

[57] F. Matera, "Fermion pairing in bose-fermi mixtures," Phys. Rev. A **68**, 043624 (2003).

[58] Daw-Wei Wang, "Strong-coupling theory for the superfluidity of bose-fermi mixtures," Phys. Rev. Lett. **96**, 140404 (2006).

[59] Ryan M. Kalas, Alexander V. Balatsky, and Dmitry Mozyrsky, "Odd-frequency pairing in a binary mixture of bosonic and fermionic cold atoms," Phys. Rev. B **78**, 184513 (2008).

[60] T. Enss and W. Zwerger, "Superfluidity near phase separation in Bose-Fermi mixtures," The European Physical Journal B **68**, 383–389 (2009).

[61] M.Yu. Kagan, I.V. Brodsky, D.V. Efremov, and A.V. Klaptsov, "Composite fermions, trios, and quartets in the Fermi-Bose mixture of neutral particles," Journal of Experimental and Theoretical Physics **99**, 640–646 (2004).

[62] Fabrizio Illuminati and Alexander Albus, "High-temperature atomic superfluidity in lattice bose-fermi mixtures," Phys. Rev. Lett. **93**, 090406 (2004).

[63] Peter Anders, Philipp Werner, Matthias Troyer, Manfred Sigrist, and Lode Pollet, "From the cooper problem to canted supersolids in Bose-fermi mixtures," Physical Review Letters **109** (2012), 10.1103/physrevlett.109.206401.

[64] Marin Bukov and Lode Pollet, "Mean-field phase diagram of the Bose-fermi hubbard model," Phys. Rev. B **89** (2014), 10.1103/physrevb.89.094502.

[65] L. Mathey, S.-W. Tsai, and A. Neto, "Competing types of order in two-dimensional Bose-fermi mixtures," Physical Review Letters **97** (2006), 10.1103/physrevlett.97.030601.

[66] M. Hettler, A. Tahvildar-Zadeh, M. Jarrell, T. Pruschke, and H. Krishnamurthy, "Nonlocal dynamical correlations of strongly interacting electron systems," Phys. Rev. B **58**, R7475–R7479 (1998).

[67] M. Jarrell, Th. Maier, C. Huscroft, and S. Moukouri, "Quantum Monte Carlo algorithm for nonlocal corrections to the dynamical mean-field approximation," Phys. Rev. B **64** (2001), 10.1103/physrevb.64.195130.

[68] Thomas Maier, Mark Jarrell, Thomas Pruschke, and Matthias Hettler, "Quantum cluster theories," Rev. Mod. Phys. **77**, 1027–1080 (2005).

[69] A. N. Rubtsov and A. I. Lichtenstein, "Continuous-time quantum Monte Carlo method for fermions: Beyond auxiliary field framework," Journal of Experimental and Theoretical Physics Letters **80**, 61–65 (2004).

[70] A. Rubtsov, V. Savkin, and A. Lichtenstein, "Continuous-time quantum Monte Carlo method for fermions," Phys. Rev. B **72** (2005), 10.1103/physrevb.72.035122.

[71] F. Assaad and T. Lang, "Diagrammatic determinantal quantum Monte Carlo methods: Projective schemes and applications to the hubbard-holstein model," Phys. Rev. B **76** (2007), 10.1103/physrevb.76.035116.

[72] T. Maier, M. Jarrell, T. Schulthess, P. Kent, and

J. White, "Systematic study of d-wave superconductivity in the 2D repulsive hubbard model," Physical Review Letters **95** (2005), 10.1103/physrevlett.95.237001.

[73] A. A. Abrikosov, *Methods of Quantum Field Theory in Statistical Physics (Dover Books on Physics)*, revised ed. (Dover Publications, 1975).

[74] A. B. Migdal, "Interaction between electrons and lattice vibrations in a normal metal," Sov. Phys. JETP **7**, 996–1001 (1958).

[75] G. M. Eliashberg, "Interactions between electrons and lattice vibrations in a superconductor," Sov. Phys. JETP **11** (1960).

[76] J. P. Carbotte, "Properties of boson-exchange superconductors," Rev. Mod. Phys. **62**, 1027–1157 (1990).

[77] F. Marsiglio and J.P. Carbotte, "Electron-phonon superconductivity," in *Superconductivity*, edited by K.H. Bennemann and JohnB. Ketterson (Springer Berlin Heidelberg, 2008) p. 73–162.

[78] Johannes Bauer, Jong E. Han, and Olle Gunnarsson, "Quantitative reliability study of the migdal-eliashberg theory for strong electron-phonon coupling in superconductors," Phys. Rev. B **84**, 184531 (2011).

[79] E. R. Margine and F. Giustino, "Anisotropic migdal-eliashberg theory using wannier functions," Phys. Rev. B **87**, 024505 (2013).

[80] B Bauer, L D Carr, H G Evertz, A Feiguin, J Freire, S Fuchs, L Gamper, J Gukelberger, E Gull, S Guertler, A Hehn, R Igarashi, S V Isakov, D Koop, P N Ma, P Mates, H Matsuo, O Parcollet, G Pawłowski, J D Picon, L Pollet, E Santos, V W Scarola, U Schollwöck, C Silva, B Surer, S Todo, S Trebst, M Troyer, M L Wall, P Werner, and S Wessel, "The alps project release 2.0: open source software for strongly correlated systems," Journal of Statistical Mechanics: Theory and Experiment **2011**, P05001 (2011).

[81] E. Gull, P. Werner, S. Fuchs, B. Surer, T. Pruschke, and M. Troyer, "Continuous-time quantum Monte Carlo impurity solvers," Computer Physics Communications **182**, 1078–1082 (2011).